Microporous and Mesoporous Materials 151 (2012) 107–112

Contents lists available at SciVerse ScienceDirect

Microporous and Mesoporous Materials

journal homepage: www.elsevier.com/locate/micromeso

Synthesis of ordered mesoporous MFI zeolite using CMK carbon templates

Hae Sung Cho [a], Ryong Ryoo [a,b,*]

[a] Center for Functional Nanomaterials, Department of Chemistry, KAIST, Daejeon 305-701, Republic of Korea
[b] Graduate School of Nanoscience and Technology (WCU), KAIST, Daejeon 305-701, Republic of Korea

ARTICLE INFO

Article history:
Received 30 August 2011
Received in revised form 3 November 2011
Accepted 4 November 2011
Available online 13 November 2011

Keywords:
Ordered mesoporous MFI zeolite
Hard template
Dry-gel synthesis
Humidity control
Template structure

ABSTRACT

Suitability of the 'dry-gel synthesis method' has been investigated for the synthesis of ordered mesoporous MFI zeolite using CMK-type mesoporous carbons as a template. Ordered mesoporous carbons with various pore diameters and topologies were infiltrated with a zeolite precursor sol, which was composed of tetrapropylammonium hydroxide, tetraethoxysilane, aluminum isopropoxide and H_2O. The porous carbon with the zeolite precursor was heated inside an autoclave under a controlled humidity condition at 443 K. The resultant product indicated that the zeolite precursor migrated onto the external surface of the carbon template to form a bulk zeolite when the relative humidity was excessively high (≥95%). A highly ordered mesoporous zeolite was synthesized in a carbon template with 10-nm pores when the humidity was lowered to 80–85%. A crystalline zeolite framework was not generated in the case of 2.5-nm pores with rigid walls. When a CMK-3 carbon with 4-nm pores was used as the template, the template walls were destroyed so that the zeolite crystalline domain was several times larger than the diameter of a single pore. Thus, humidity, template pore diameters and framework rigidity should be taken into account for application of the dry-gel synthesis method.

1. Introduction

Mesoporous aluminosilicate materials with a crystalline microporous framework have recently garnered much attention for their potential to resolve diffusion and mass transfer limitations of microporous zeolites [1,2]. Mesopores can be generated in a zeolite via treatment with an acid or alkali solution that partially leaches aluminum or silicon from the zeolite framework [3–5]. Although the demetallation method is suitable for a large-scale practical process, its applicability depends heavily on structures of the zeolite framework and Si/Al ratios. Moreover, the chemical leaching process can drastically deteriorate both the framework crystallinity and the morphology in the process of increasing mesoporosity. Normally, mesopore diameters obtained in this manner are not uniform. Instead, zeolite synthesis methods using templates are suitable for generating uniform mesopores. Mesopore-generating templates can be classified into two groups: (1) soft templates including surfactants, polymers and starch [6–13], and (2) hard templates such as polystyrene beads, carbon black, carbon nanotubes and wood cells [14–17]. Employing these templates, zeolite crystals can be grown within a limited space confined by the template pore walls. The templates can be removed after the zeolite crystallization through a combustion process.

Ordered mesoporous carbons have drawn attention as a template for zeolite as they are readily available with various pore structures with controlled diameters [18,19]. Carbon with a 3-dimensional network of mesopores is suitable for the synthesis of mesoporous zeolite. The carbon mesopores can be infiltrated with a zeolite precursor sol, composed of, for example, tetrapropylammonium hydroxide (TPAOH), tetraethoxysilane (TEOS), aluminum isopropoxide and H_2O. It is also possible to infiltrate TPAOH and H_2O into a silica/carbon nanocomposite material, if the composite has sufficient porosity for infiltration [20]. The carbon template containing the zeolite precursor can then be heated in an autoclave until the zeolite is crystallized. Finally, the zeolite product can be released by combustion of the carbon template. A highly ordered mesoporous zeolite can be obtained in principle, if the zeolite precursor can be transformed into a continuous network of crystalline zeolite phase in the carbon template. However, in practice, it is very difficult to control zeolite crystallization to occur in such a confined manner inside narrow mesoporous channels. Generally, zeolite precursors tend to migrate from mesopores to external surfaces during the course of zeolite crystallization. This results in the formation of bulk zeolite crystals separately from the carbon template.

A steam-assisted dry-gel conversion method is often used to resolve the zeolite separation problem from carbon [21–26]. In the 'dry-gel synthesis', the zeolite precursor is converted to a nonvolatile gel state within the template pores. The template-gel

* Corresponding author at: Center for Functional Nanomaterials, Department of Chemistry, KAIST, Daejeon 305-701, Republic of Korea. Tel.: +82 42 350 2830; fax: +82 42 350 8130.
E-mail address: rryoo@kaist.ac.kr (R. Ryoo).

1387-1811/$ - see front matter © 2011 Elsevier Inc. All rights reserved.
doi:10.1016/j.micromeso.2011.11.007

composite is dried by complete evaporation of the solvent (or moisture), and subsequently heated in an autoclave containing a limited amount of water placed on the bottom of the autoclave. The dry-gel method was originally developed as a means of pseudomorphic conversion of a gel-type zeolite precursor into a zeolite sample with a similar shape. The synthesis method was applied in recent years to zeolite syntheses using porous carbon templates. Compared with conventional hydrothermal synthesis, the zeolite precursor was not in direct contact with the aqueous phase. Hence, the dry-gel method is often believed to prevent migration of the zeolite precursor from the carbon templates. Fang and Hu [25] claimed the synthesis of a highly ordered mesoporous material with zeolitic pore walls, via the dry-gel conversion of silica/CMK-5 carbon composite (silica is located within carbon pores of 3–5 nm in diameter). Their claim was based on X-ray diffraction (XRD) patterns and nitrogen adsorption isotherms. These results indicated the simultaneous presence of an ordered mesoporous phase and crystalline microporous zeolite at the same time in the product. However, the characterization data could not completely resolve whether the product was indeed a crystalline zeolite with a well ordered mesoporous structure, or a mixture of bulk zeolite crystals and amorphous silica phase. We attempted to reproduce the synthesis in our laboratory, but failed. More recently, Fan et al. reported on the synthesis of MFI zeolite exhibiting ordered mesoporosity, using carbon templates that were synthesized by replication of colloidal silica nanoparticles (10–40 nm in diameter) [26]. In this case, the formation of the mesoporous structure with a crystalline zeolite framework was indeed verified by a high-resolution transmission electron microscopic (TEM) analysis.

It can be reasonably anticipated that dry-gel zeolite synthesis using a hard template would become progressively more difficult as the pore diameter decreases to the extremely small limit. The zeolite crystallization would be affected by the template pore topologies as well as pore diameters. These effects would be altered by the humidity of the zeolite synthesis chamber. However, such effects have not been systematically investigated thus far. Hence, in the present study, we investigated the crystallization of MFI zeolite using ordered mesoporous carbon templates with various pore diameters and topologies. We followed the dry-gel conversion method under various relative humidity conditions. In most previous works, humidity was controlled by the amount of water placed in the autoclave, and it was difficult to ascertain the exact value. Naik et al. [27] designed a reactor that could control the relative humidity by the temperature difference between the sample and water regions inside the autoclave. In the present work, the relative humidity was precisely controlled by the concentration of salt in the water region, using Raoult's law. A complementary combination of TEM and scanning electron microscope (SEM), X-ray diffraction (XRD) and nitrogen adsorption was used to investigate the effects of humidity and pore structures on the crystallization of MFI zeolite inside a carbon template. The results were extended to optimize the zeolite synthesis conditions.

2. Experimental section

2.1. Materials

Mesoporous silicas and carbon samples were prepared following the synthesis procedures reported in the literature [28–31]. Briefly, a mesoporous silica sample of SBA-15 silica (hexagonal *p*6*mm* structure) was synthesized with tetraethylorthosilicate (TEOS) and Pluronic P123 surfactant under the hydrothermal synthesis condition at 423 K [28]. An MCM-48 silica sample (cubic *Ia*3*d* structure) was synthesized with a sodium silicate solution (9 wt.% aqueous solution, Na/Si = 0.5) and hexadecyltrimethylammonium bromide at 373 K [29]. A KIT-6 silica (cubic *Ia*3*d* structure with large mesopore) was synthesized with TEOS and Pluronic P123 surfactant at 308 K using *n*-butanol as a co-structure-directing agent [30]. A CMK-1 carbon (tetragonal $I4_1/a$ structure) was synthesized with sucrose using MCM-48 as a template via the established procedure [31]. A CMK-3 carbon was prepared from furfuryl alcohol carbon precursor and SBA-15 [28]. A CMK-type carbon was synthesized with furfuryl alcohol using the KIT-6 silica as a template [30]. This carbon had a tetragonal $I4_1/a$ structure similar to that of CMK-1, but the mesopore diameters were much larger (*ca.* 10 nm). This carbon is designated as 'CMK-L', where 'L' denotes 'large pores'.

Zeolite synthesis using carbon templates was performed as follows: tetrapropylammonium hydroxide (TPAOH, 20–25 wt.% in aqueous solution), TEOS and aluminum isopropoxide [$Al(OC_3H_7)_3$] were stirred until a homogeneous solution was obtained. The $Al(OC_3H_7)_3$/TPAOH/TEOS molar ratios were in a range of [0–2]:25:100. A portion of this solution was mixed with a carbon template such that the volume of the solution was exactly twice that of the total pore volume of the carbon. The resultant sample was dried slowly in a rotary evaporator at 313 K so that EtOH (generated from TEOS) and H_2O were fully removed. Subsequently, the sample was infiltrated again with an additional amount of TPAOH–TEOS solution. The solution-to-carbon pore volume ratio was 1.00 in the second infiltration. The sample was dried again in a rotary evaporator. The resultant sample was placed into a small Pyrex vial, which was mounted in the middle of a Teflon-lined autoclave. A sufficient amount of aqueous ammonium nitrate solution was placed at the bottom of the autoclave, preventing physical contact with the sample. Humidity was controlled by the molar ratio of water to total solution, established by Raoult's Law. After heating the autoclave at 443 K for 6 d under a static condition, the sample was collected. Finally, the sample was calcined at 873 K in air for 6 h. The sample obtained in this manner is denoted as $Al_xSi_{1-x}O_2$/CMK-*n*. Here, '*x*' indicates the Al molar fraction in the aluminosilicate product and CMK-*n* is the carbon template.

For hydrothermal synthesis of Silicalite-1, TPAOH and TEOS were dissolved in distilled water to obtain a molar composition of 1 TPAOH/4 SiO_2/360 H_2O. The transparent solution was further aged for 2 h at room temperature under magnetic stirring. Subsequently, the gel mixture was transferred to a Teflon-coated stainless-steel autoclave and hydrothermally treated at 443 K under static condition. After zeolite crystallization for 2 d, the precipitated solid product was filtered, washed with distilled water, and dried in an oven at 373 K. The as-synthesized silicalite-1 product was calcined in air for 6 h at 873 K for organic removal.

2.2. Characterization

Powder XRD patterns in the region of $2\theta \leq 3^\circ$ were recorded in the reflection mode (λ = 0.154250 nm) using synchrotron radiation at BL8C2 of the Pohang Light Source. XRD measurement was performed at steps of 0.005° with an accumulation time of 0.5 s per step under ambient conditions. Powder XRD patterns for $2\theta > 3^\circ$ were record with a Rigaku Multiflex diffractometer using a monochromatized X-ray beam from nickel-filtered Cu Kα radiation (40 kV, 40 mA). The XRD step scan was performed under ambient conditions at steps of 0.02° and an accumulation time of 0.5 s per step SEM images were obtained using a Hitachi S-4800 scanning electron microscope with a field emission gun. The powder sample was dispersed on a carbon tape support without metal coating. For TEM imaging, the powder sample was suspended in acetone (99.5 vol.%) by ultrasonication. The acetone was dropped and evaporated on a carbon microgrid. The imaging was performed at room temperature using a Tecnai F30 operated at 300 kV. Nitrogen adsorption–desorption isotherms were measured at 77 K, using a volumetric gas sorption analyzer (Quantachrome AS-1MP). Prior

to the adsorption measurements, samples were outgassed for 2 h at 623 K. The Brunauer–Emmett–Teller (BET) equation was used to calculate the specific surface area, from the adsorption data in the region of $0.05 < P/P_0 < 0.2$. The micropore volume was calculated by a Saito–Foley analysis [32], and the mesopore volume was calculated by subtracting the micropore volume from the total pore volume measured at $P/P_0 = 0.97$. Pore size distribution was calculated from the adsorption branch of the N_2 isotherm using the Barret–Joyner–Halenda (BJH) method [33].

3. Results and discussion

3.1. Effect of chamber humidity on crystallization of MFI zeolite in carbon template

The effect of humidity has been investigated for the dry-gel synthesis of siliceous MFI zeolite using CMK-L carbon. The pore diameters of this carbon (10 nm as determined by the BJH method) were approximately 5 times greater than the longest crystal lattice dimension of the MFI zeolite. The mesopore walls were approximately 5.1 nm thick. This carbon was chosen as a template in this investigation because the mesopores were thought to be sufficiently large for the formation of the zeolite crystal, and pore walls were sufficiently rigid. The zeolite was allowed to crystallize for 6 d at 443 K under various humidity levels ranging from 30% to 100%. Figs. 1 and 2 show powder XRD patterns, SEM images and TEM images of the resultant products, i.e., the template-free silica products synthesized in this manner. Fig. 1A presents the XRD patterns for the silica sample obtained at 30% humidity. The small-angle pattern shows quite a few well-resolved diffractions, which were characteristic of the ordered mesoporous structure corresponding to the CMK-L template. However, no diffractions characteristic of a crystalline zeolitic structure could be detected in the wide-angle region. A broad background peak appeared in the 2θ range of 20–30°, indicating that the silica frameworks were completely amorphous. No MFI zeolite phase was detected by XRD even after 2 weeks of time was given for crystallization.

The wide-angle XRD pattern in Fig. 1B shows that the zeolite began to crystallize when the humidity was increased to 50%. The XRD pattern in Fig. 1C shows that the crystallinity was increased more conspicuously when the humidity was increased to 85%. The detailed structures of this sample were investigated by high-resolution TEM and SEM. As shown in the high resolution SEM image in Fig. 2A, the silica sample synthesized at 85% relative humidity exhibited regularly corrugated surface morphologies, which are characteristic of a highly mesoporous material. The sample contained very few particles without such surface corrugation indicating the formation of bulk zeolite. From the low-resolution TEM image, it was confirmed that the sample was a highly ordered mesoporous material corresponding to a faithful replication of its CMK-L template. Furthermore, the lattice fringes in the high resolution TEM image (Fig. 2D) clarified that the mesoporous structure was composed of crystalline frameworks of the MFI zeolite. The ordered mesoporous zeolite was easily distinguished from other ordered mesoporous silicas with amorphous silica frameworks such as SBA-15 and MCM-41. The resolved diffractions in the small-angle XRD pattern in Fig. 1C originate from the structural coherences between zeolite walls in the regular arrangement of the ordered mesoporous architecture. This indicates that the zeolite precursor could completely transform to crystalline zeolite inside the carbon template mesopores at 85% relative humidity.

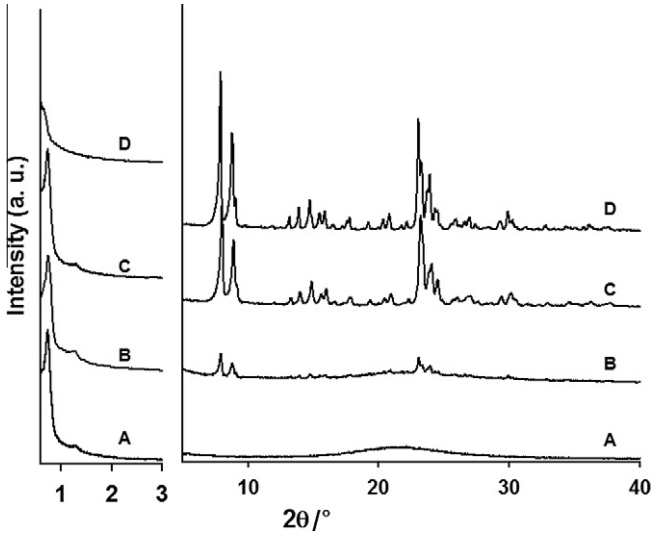

Fig. 1. Powder XRD patterns of MFI zeolites (SiO_2/CMK-L), synthesized by following dry-gel conversion method at (A) 30%, (B) 50%, (C) 85%, and (D) 100% relative humidity.

Bulk zeolite crystals were obtained when the humidity was further increased to 100%. The resultant SEM image in Fig. 2B shows the morphologies for a bulk zeolite crystal without mesoporosity. From this result, it turned out that the zeolite precursor totally migrated from the mesopores of the carbon template to its external surfaces during the synthesis at 100% humidity. The migration of the zeolite precursor could be suppressed more effectively by lowering the humidity. However, at low humidity below 50%, it appeared that the vapor pressure of water was not high enough to transform the precursor to the zeolite phase. The amount of water vapor must be high enough to transform the zeolite precursor to the zeolite crystals, but low enough to prevent escape of the zeolite precursor from the template pores. From the results, it may be concluded that 85% relative humidity was an optimum condition for the synthesis of pure-silica MFI zeolite inside a mesoporous carbon template. Indeed, the zeolite product synthesized at 85% humidity exhibited both an ordered mesoporous structure and crystalline MFI zeolite frameworks.

Fig. 3 shows the nitrogen adsorption isotherm of the zeolite sample synthesized at 85% humidity, along with that of a bulk MFI zeolite of the same composition (Silicalite-1) for comparison. The adsorption branch was used to analyze the pore size distribution. Both the bulk Silicalite-1 zeolite and mesoporous MFI sample exhibited a step-wise increase in the adsorption at low partial pressure ($P/P_0 \approx 0.2$). This adsorption corresponded with an apparently sharp peak at 2 nm in the pore size distribution. However, this peak was not due to the presence of 2-nm pores. As discussed in previous studies, the adsorption jump at $P/P_0 \approx 0.2$ can be explained by a phase transformation of the adsorbed nitrogen from a disordered fluid phase to a more ordered crystalline phase [32,34], or by a systematic structural transition of the MFI zeolite framework from monoclinic to orthorhombic as a result of nitrogen adsorption [35]. The bulk zeolite sample exhibited no other peaks in the pore size distribution. On the other hand, the mesoporous MFI zeolite prepared at 85% relative humidity shows an additional large increase in the adsorption with a hysteresis loop in the range of $P/P_0 = 0.7–0.9$. This is due to capillary condensation in the mesopores. The mesopore size analysis by the BJH method gave a narrow peak centered at a diameter of 8.7 nm. The presence of these mesopores in the crystalline zeolite is consistent with the electron microscopy data noted above. Due to the mesopores, the zeolite sample exhibited a high specific BET surface area and total pore volume as compared to the bulk zeolite. The micropore volume of SiO_2/CMK-L prepared at 85% relative humidity was 0.11 cm^3/g, which is similar to that of conventional Silicalite-1. However, as the relative humidity decreased to 50%, the micropore volume and BET surface area of the resultant zeolite product

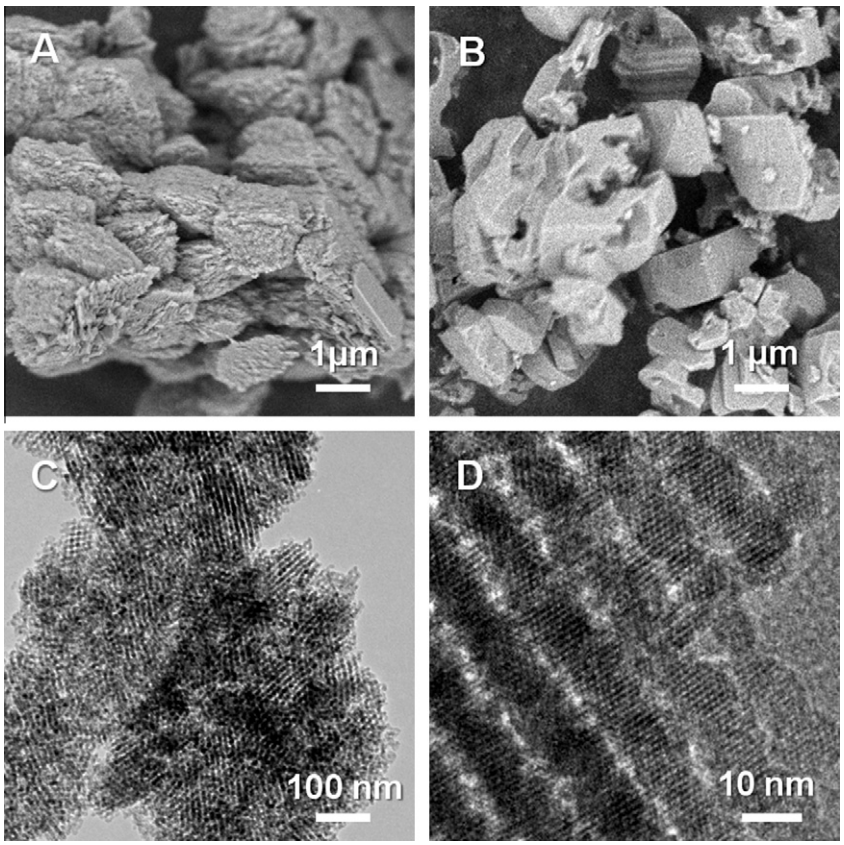

Fig. 2. SEM micrographs of SiO_2/CMK-L at (A) 85%, (B) 100% relative humidity and TEM images of (C, D) SiO_2/CMK-L at 85% relative humidity.

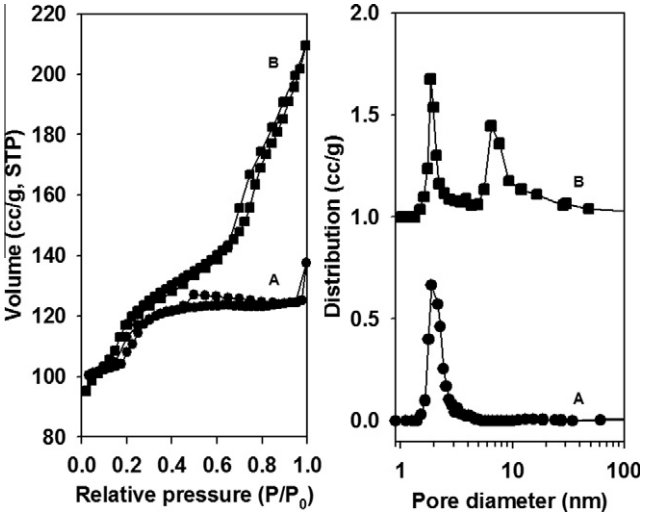

Fig. 3. Nitrogen adsorption isotherms and pore size distributions of (A) Silicalite-1 and (B) SiO_2/CMK-L at 85% relative humidity. The pore size distribution for SiO_2/CMK-L at 85% humidity was vertically offset by 1 cm^3/g.

decreased (0.09 cm^3/g and 263 m^2/g). These results indicate that the relative humidity could be an important variable for full crystallization of zeolite, as has been previously described [27]. The pore textural properties are summarized in Table 1.

3.2. Ordered mesoporous MFI zeolite with different Si/Al ratios

In general, crystallization of MFI zeolite takes longer time as the Al content is increased (or with lowering of the Si/Al ratio). Further, the initial synthesis gel becomes more viscous. These changes progressively impede the infiltration of the zeolite precursor into template pores. It is also noteworthy that the zeolite synthesis gel becomes more hygroscopic with increasing Al content. We investigated the effects of Si/Al ratio, considering these three factors for the synthesis of aluminosilicate MFI zeolite in a CMK-L template. The zeolite precursor had to be added into the carbon template in a clear solution (or sol) state before gelation, in order to achieve uniform infiltration into the carbon mesopores. This places a limitation for the Si/Al molar ratio within a range of 50–∞. In the case of Si/Al < 50, the template synthesis failed because the zeolite precursor was immediately polymerized into a gel as soon as the raw materials were mixed. Highly ordered mesoporous MFI zeolite was successfully prepared at 70% relative humidity when the Si/Al ratio was 100. The optimum humidity had to be lowered to 60% at the Si/Al ratio of 50. These changes in the optimum humidity appeared to be related to the increasingly hygroscopic nature of the aluminosilicate gel. It is reasonable that the H_2O content in the synthesis gel would increase as the Al content increased under the same relative humidity. Due to the high H_2O content, it appeared that the zeolite precursors could transform to zeolite crystals more easily than in the synthesis of pure silica MFI. However, at the same time, the high H_2O content facilitated migration of the zeolite precursor from the template pores to the external surfaces. It is then reasonable that the optimum humidity should be lowered to compensate the effect of the Al content.

The structure of the MFI samples with Si/Al = 50 and 100 was characterized by TEM, SEM and XRD. These structural investigations confirmed that the aluminosilicate samples had a well-ordered mesoporous structure with a highly crystalline MFI zeolite framework, similar to that of the pure silica sample obtained under the optimized synthesis condition. For instance, as shown in Fig. 4, mesoporous MFI products with different Si/Al ratios exhibited very

Table 1
Pore structural parameters of MFI zeolites synthesized by following a conventional and dry-gel conversion method.

Sample[a]	S_{BET}[b] (m^2/g)	V_{micro}[c] (cm^3/g)	V_{meso}[d] (cm^3/g)	V_t[e] (cm^3/g)	D_{BJH}[f] (nm)
Silicalite-1	298	0.14	0.02	0.16	–
SiO_2/CMK-L (85% humidity)	350	0.14	0.17	0.31	8.7

[a] Silicalite-1 was prepared by following the conventional synthesis procedure for MFI zeolite and SiO_2/CMK-L was synthesized by the steam-assisted dry-gel conversion method by using CMK-L as hard template.
[b] Surface area calculated using the BET method.
[c] Micropore volume calculated by Saito–Foley analysis.
[d] Mesopore volume corresponding to pore diameters in the range of 1.7–50 nm.
[e] The total pore volume at relative pressure 0.97.
[f] The mesopore diameter calculated from adsorption branch by using the BJH method.

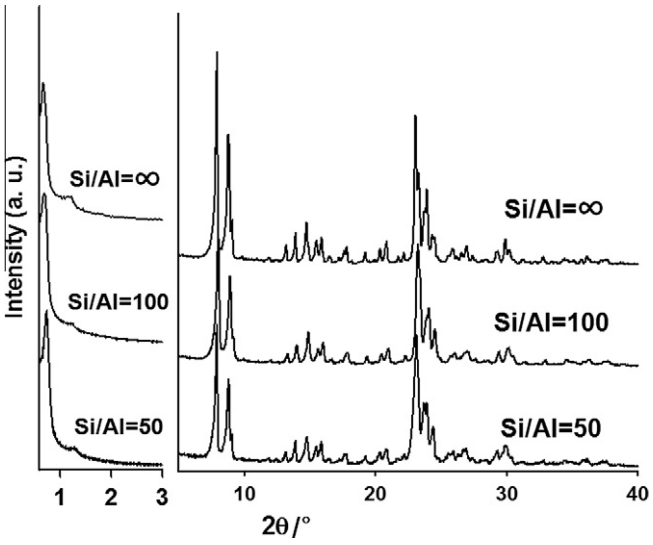

Fig. 4. Powder XRD patterns of aluminum containing MFI zeolites synthesized by using CMK-L template ($Al_xSi_{1-x}O_2$/CMK-L) with various Si/Ai ratios in the range of 50–∞.

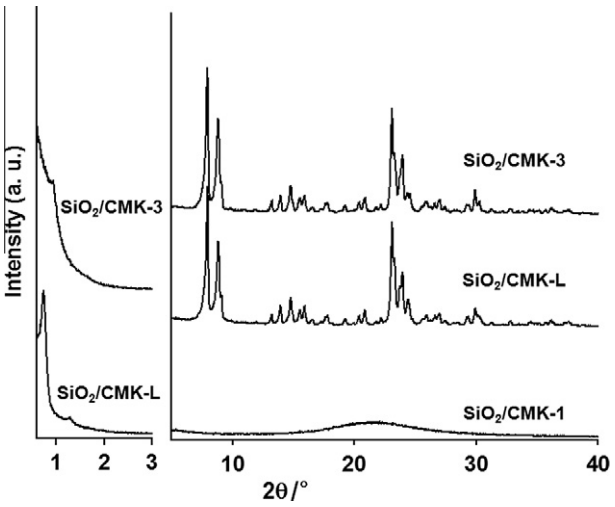

Fig. 5. XRD patterns of SiO_2/CMK-*n* samples using mesoporous carbon templates with various pore structures. The letter after hyphen '*n*' denotes the mesoporous carbon template CMK-*n*.

similar XRD patterns characteristic of both a crystalline MFI structure and a highly ordered mesoporous structure. The small-angle diffraction pattern indicated that the mesoporous zeolite had a tetragonal $I4_1/a$ structure, which corresponded to the structure of the CMK-L carbon. TEM investigation of the zeolite product with Si/Al = 50 clarified the ordered mesoporosity and framework crystallinity (see Supplementary Information Fig. S1). The nitrogen adsorption isotherm of $Al_{0.02}Si_{0.98}O_2$/CMK-L exhibited a type-IV isotherm with an additional capillary condensation step in the mesopores compared to the ZSM-5 (Si/Al = 50) (Fig. S2, Table S1).

3.3. Effect of mesoporous structure of hard template

The effect of the mesoporous structure of hard template has been investigated through an attempt to synthesize pure silica MFI zeolites at 85% relative humidity, using ordered mesoporous carbon materials with two different structures, CMK-1 and CMK-3, as templates. CMK-1 had the same pore topology as CMK-L, belonging to the same tetragonal $I4_1/a$ space group, but had much smaller mesopores (2.5 nm in diameter) and thinner walls (4.0 nm thick). Note that the pore diameter was 10 nm, and the wall thickness was 5.1 nm in the case of CMK-L. Unlike the successful synthesis of a highly ordered mesoporous zeolite using CMK-L, the synthesis attempt using CMK-1 failed to yield a zeolite at 85% humidity. The small-angle XRD pattern in Fig. 5 exhibits well-resolved diffractions, indicating that the silica sample was a faithful replica of the ordered mesoporous structure of the carbon template. However, the wide-angle pattern was featureless with a broad background in the 2θ region of 17–28° even after 16 days of time was given for zeolite crystallization at 443 K. Thus, the product was mesoporous silica without framework crystallinity. The lack of zeolite crystallization in this case is believed to be a result of the very small pore diameter of the template. It was reported that a 2.8-nm sized aggregation of primary building units is an essential step in the nucleation process for crystallization of MFI zeolite [36]. If this principle is also applied to dry-gel synthesis using a template, the pore diameters should be greater than the minimum size requirement for the initial zeolite domain. The zeolite crystallization within the mesopore channel of CMK-1 appeared to be unsuccessful due to the small mesopore diameter (2.5 nm) as previously reported [19].

The CMK-3 carbon used in this work had a bundle-like arrangement of carbon nanorods according to the 2-dimensionally hexagonal structure. The carbon rods were approximately 4.2 nm in diameter, and the rods were rigidly supported by short bridges. The interconnecting carbon bridges are very thin, corresponding to the micropore diameter of mesoporous silica template [37]. The space between carbon rods corresponding to mesopores was approximately 3.1 nm in diameter. These mesopores were used as a template in the pure silica MFI zeolite under the 85% relative humidity condition. As the XRD pattern in Fig. 5 shows, the product from the CMK-3 template exhibited a wide-angle XRD pattern for well-crystalline MFI zeolite. However, the small-angle pattern indicated that this zeolite sample had a poor structural order in mesoscale. Despite the loss of mesostructural order, the zeolite sample gave a nitrogen adsorption isotherm with a very steep jump of adsorption quantity in the range of P/P_0 = 0.7–0.9 (see Supplementary Information Fig. S3). This adsorption indicated capillary

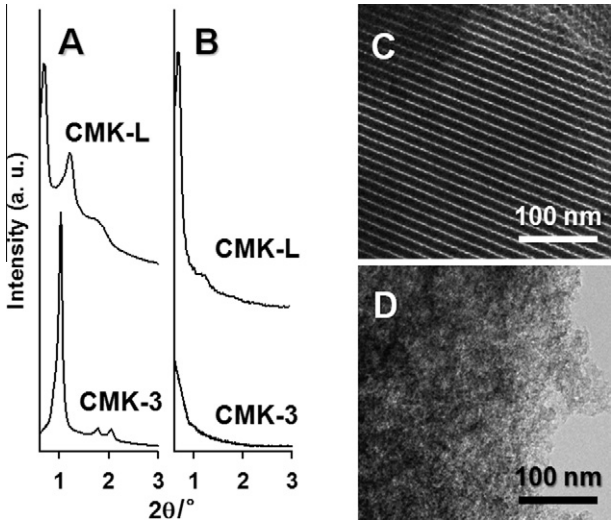

Fig. 6. XRD patterns of (A) carbon templates before zeolite crystallization, (B) after crystallization and TEM micrographs of (C) CMK-L, and (D) CMK-3 after crystallization.

condensation of nitrogen in mesopores about 29.9 nm in diameter. These mesopores could be confirmed in the TEM image (see Supplementary Information Fig. S4). However, the mesopores were present in a disordered manner at the intercrystalline space between zeolite nanocrystals. The nanoparticles were larger than the template pore diameters. This indicates that the template pore walls were destroyed when zeolite crystallization occurred. It is believed that the zeolite precursor gel can be dissolved by condensed water in the mesopores of the carbon template, transforming into zeolite crystals with structural rearrangement [38]. The pore walls should be thick enough to prevent excessive growth of zeolite crystals. In the case of the present CMK-3 template, it appeared that the short carbon bridges supporting the main carbon nanorods were not rigid enough to prevent crystal growth. The crystal growth could cause destruction of the carbon template and the formation of zeolite nanoparticles in a disordered manner. Compared to CMK-3, cubic *Ia*3*d* mesoporous silica consisting of a disconnected enantiomeric pair of mesopores is used as a template for the synthesis of CMK-L. Therefore, the mesoporous carbon template without thin carbon bridges could support mesostructural ordering of the zeolite during the zeolite crystallization. To confirm the structural change of the template during zeolite crystallization, the carbon template after zeolite crystallization was studied by XRD and TEM (Fig. 6). The zeolite phase within the carbon template was removed by HF washing. In the case of the CMK-L template, the carbon framework was well retained after zeolite crystallization process. However, in the case of CMK-3, the carbon framework was destroyed during zeolite crystallization. From these results, it is concluded that the mesopore diameter and wall thickness of the carbon template are important factors for zeolite crystallization and preservation of the original mesostructural ordering of the carbon template.

4. Conclusion

In conclusion, synthesis of MFI zeolites by following a steam-assisted dry-gel conversion method and using CMK carbon templates was studied under various synthesis conditions such as humidity, aluminum content and structure of the carbon template. It is found in this study that the relative humidity and mesoporous structure of the ordered mesoporous carbon template play important roles in crystallization within the mesopore channel of templates and the preservation of an ordered mesoporous structure. From the structural investigation of a SiO_2/CMK-L product at 85% humidity, it is confirmed that the product has a well ordered mesostructure with crystalline zeolite frameworks. In addition, preparation of ordered mesoporous MFI zeolite with various Si/Al ratios was successfully performed. Furthermore, the approach used in the present study of the effects of humidity, template pore diameter and framework rigidity on the crystallization of mesoporous MFI zeolite could be applied to other inorganic materials possessing diverse compositions and crystalline structures.

Acknowledgments

This work was supported by the National Honor Scientist Program (20100029665) and World Class University Program (R31-2010-000-10071-0) of the Ministry of Education, Science, and Technology in Korea. Synchrotron radiation XRD was conducted at Pohang Light Source (2007-3086-16).

Appendix A. Supplementary data

Supplementary data associated with this article can be found, in the online version, at doi:10.1016/j.micromeso.2011.11.007.

References

[1] M. Hartmann, Angew. Chem., Int. Ed. 43 (2004) 5880.
[2] Y. Tao, H. Kanoh, L. Abrams, K. Kaneko, Chem. Rev. 106 (2006) 896.
[3] A. Corma, V. Fornes, S.B. Pergher, Th.L.M. Maesen, J.G. Buglass, Nature 96 (1998) 353.
[4] J.C. Groen, J.C. Jansen, J.A. Moulijn, J. Perez-Ramirez, J. Phys. Chem. B 108 (2004) 13062.
[5] J.C. Groen, J.A. Moulijn, J. Perez-Ramirez, J. Mater. Chem. 16 (2006) 2121.
[6] J.S. Beck, J.C. Vartuli, G.J. Kennedy, C.T. Kresge, W.J. Roth, S.E. Schramm, Chem. Mater. 6 (1994) 1816.
[7] A. Karlsson, M. Stöcker, R. Schmidt, Micropor. Mesopor. Mater. 27 (1999) 181.
[8] N. Petkov, M. Hölzl, T.H. Metzger, S. Mintova, T. Bein, J. Phys. Chem. B 109 (2005) 4485.
[9] M. Choi, H.S. Cho, R. Srivastava, C. Venkatesan, D.H. Choi, R. Ryoo, Nat. Mater. 5 (2006) 728.
[10] M. Choi, K. Na, J. Kim, Y. Sakamoto, O. Terasaki, R. Ryoo, Nature 461 (2009) 728.
[11] H.T. Wang, B.A. Holmberg, Y.S. Yan, J. Am. Chem. Soc. 125 (2003) 9928.
[12] J. Yao, H. Wang, S.P. Ringer, K.Y. Chan, L. Zhang, N. Xu, Micropor. Mesopor. Mater. 85 (2005) 267.
[13] M.B. Yue, L.B. Sun, T.T. Zhuang, X. Dong, Y. Chun, J.H. Zhu, J. Mater. Chem. 18 (2008) 2044.
[14] C.J.H. Jacobsen, C. Madsen, J. Houzvicka, I. Schmidt, A.J. Carlsson, J. Am. Chem. Soc. 122 (2000) 7116.
[15] B.T. Holland, L. Abrams, A. Stein, J. Am. Chem. Soc. 121 (1999) 4308.
[16] I. Schmidt, A. Boisen, E. Gustavsson, K. Ståhl, S. Pehrson, S. Dahl, A. Carlsson, C.J.H. Jacobsen, Chem. Mater. 13 (2001) 4416.
[17] A. Dong, Y. Wang, Y. Tang, N. Ren, Y. Zhang, Y. Yue, Z. Gao, Adv. Mater. 14 (2002) 926.
[18] Y.S. Tao, H. Kanoh, L. Abrams, K. Kaneko, Chem. Rev. 106 (2006) 896.
[19] Z.X. Yang, T.D. Xia, R. Mokaya, Adv. Mater. 16 (2004) 727.
[20] S. Tanaka, C. Yuan, Y. Miyake, Micropor. Mesopor. Mater. 113 (2008) 418.
[21] S.I. Cho, S.D. Choi, J.H. Kim, G.J. Kim, Adv. Funct. Mater. 14 (2004) 49.
[22] A. Sakthivel, W.H. Chen, R. Ryoo, S.B. Liu, Chem. Mater. 16 (2004) 3168.
[23] M. Ogura, Y. Zhang, S.P. Elangovan, T. Okubo, Micropor. Mesopor. Mater. 101 (2007) 224.
[24] Y. Zhang, T. Okubo, M. Ogura, Chem. Commun. (2005) 2719.
[25] Y. Fang, H. Hu, J. Am. Chem. Soc. 128 (2006) 10636.
[26] W. Fan, M.A. Snyder, S. Kumar, P.S. Lee, W.C. Yoo, A.V. McCormick, R.L. Penn, A. Stein, Nat. Mater. 7 (2008) 984.
[27] S.P. Naik, A.S.T. Chiang, R.W. Thompson, J. Phys. Chem. B 107 (2003) 7006.
[28] S. Jun, S.H. Joo, R. Ryoo, M. Kruk, M. Jaroniec, Z. Liu, T. Ohsuna, O. Terasaki, J. Am. Chem. Soc. 122 (2000) 10712.
[29] R. Ryoo, S.H. Joo, J.M. Kim, J. Phys. Chem. B 103 (1999) 7435.
[30] T.W. Kim, F. Kleitz, B. Paul, R. Ryoo, J. Am. Chem. Soc. 127 (2005) 7601.
[31] R. Ryoo, S.H. Joo, S. Jun, J. Phys. Chem. B 103 (1999) 7743.
[32] A. Saito, H.C. Foley, Micropor. Mater. 3 (1995) 543.
[33] E.P. Barrett, L.G. Joyner, P.P. Halenda, J. Am. Chem. Soc. 73 (1951) 373.
[34] J.C. Groen, L.A.A. Peffer, J. Perez-Ramirez, Micropor. Mesopor. Mater. 60 (2003) 1.
[35] R.J.M. Pellenq, D. Nicholson, Langmuir 11 (1995) 1626.
[36] P.P.E.A. Moor, T.P.M. Beelen, R.A. Santen, J. Phys. Chem. B 103 (1999) 1639.
[37] R. Ryoo, C.H. Ko, M. Kruk, V. Antochshuk, M. Jaroniec, J. Phys. Chem. B 104 (2000) 11465.
[38] T. Sano, Y. Kiyozumi, F. Mizukami, H. Takaya, T. Mouri, M. Watanabe, Zeolites 12 (1992) 131.